DOI 10.5012/bkcs.2010.31.10.2913

# Electrochemical Investigation of Animal Tissue Embedded Biosensor Bound with Ethylene-Propylene Rubber

**Kil-Joong Yoon**

*Division of Natural Sciences, Cheongju University, Cheongju 360-764, Korea. E-mail: kjyoon@cju.ac.kr*
*Received March 25, 2010, Accepted August 28, 2010*

When rubber dissolved in toluene was used as a binding material of graphite powder, the mechanical robustness of the carbon paste was guaranteed by the fast volatility of the solvent immediately after electrode construction. This characteristic of the rubber solution met qualifications for practical use of carbon paste electrodes and enabled the design of a new enzyme electrode bound with EPDM. In order to confirm whether the electrode shows quantitative electrochemical behaviors or not, its kinetic parameters, e. g. the symmetry factor (0.2), the exchange current density (3.66 $\mu A/cm^2$), the capacity of the double layer ($2.0 \times 10^{-5}$ F), the Michaelis constant ($4.39 \times 10^{-3}$ M), the diffusion coefficient of substrate ($2.58 \times 10^{-12}$ $cm^2$/sec), the time constant (0.018 sec) and other factors were investigated.

**Key Words**: Hydrogen peroxide, Peroxidase, Enzyme electrode, Biosensor, Chicken liver

## Introduction

Immense catalytic power and specificity are the most striking characteristics of enzymes. They accelerate reactions by factors of at least a million even at lower temperatures. Thus a good immobilization of the enzyme on the transducer surface is one of the key factors for the durable preservation and the reproducibility of the sensor system monitoring the biological process. A huge research effort for the practical use of enzyme electrode has been directed towards finding good immobilization methods for enzymes. Conventional methodologies pursued up to now include physical adsorption,[1] covalent bonding or cross-linking with multi-functional reagents,[2,3] entrapping within conducting polymer film,[4,5] mixing within the bulk composite of electrode materials, or screen printing.[6-8] Also sol-gel processing for biomedical monitoring was temporarily prevalent.[9,10] But the above techniques which go through the physical and the chemical processes of manufacture are laborious and time consuming.

Making a detour around those complications, the carbon paste method[11-13] came onto the stage. This incorporates enzymes or zymogen in the mixture of carbon powder and mineral oil and uses them as electrode materials. In this lab, many kinds of enzyme electrodes were manufactured in the same way to determine their response characteristics with hydrogen peroxide.[14-21] The advantages of the carbon paste electrode, including low cost, simplicity of manufacturing and fast response, are very useful in studying the electrochemical peculiarities of enzymes. But this method remains far from practical use because its binder, mineral oil, is nonvolatile and not rigid. Therefore, a strong need for a rigid and practicable binder made us look for a desirable binder. Rubber dissolved in toluene came into satisfied our wishes due to the fast volatility of the solvent after the electrode construction. As a result, electrodes using various kinds of rubber have been designed, their applications have been explored and our research activities revolving around this are increasing at this time. Secondly, an additional and essential requirement for the practical use of the sensor is its reproducibility and quantitative electrochemical behavior. It is known that EPDM is inert chemically and has good resistance to acids and alkali. It is especially resistant to polar solvents.[22] Holding out hope that those points will meet the requirement of a good binder, the enzyme electrode bound with EPDM was fabricated. In order to confirm whether the electrode shows quantitative electrochemical behaviors or not, its kinetic parameters were determined. The details are reported here.

## Experiment

**Reagents and measurements.** The chicken liver tissue ruptured with homogenizer was used as a source of peroxidase and discarded after a single use. Ethylene-propylene diene monomer (abbr. EPDM) was a product of KUMHO polychem (KEP-350, 7 ~ 9% diene). Toluene and graphite powder were purchased from Sigma-Aldrich (≥ 99.9%) and from Fluka (≤ 0.1 mm), respectively. Hydrogen peroxide (Junsei, EP, 35 %) for substrate (abbr. S), NaCl (Shinyopure Chem. ≥ 99.5%) for electrolyte and ferrocene (Sigma) for the mediator were used. Ag/AgCl (BAS MF 2052) and Pt electrode (BAS Mw 1032) were used for the reference and for the auxiliary electrodes, respectively. The enzyme electrode was connected to a BAS model EPSILON (Bioanalytical system, Inc/, U. S. A.) to obtain linear sweep voltammograms. The other amperometric measurements were performed with EG&G Model 362 potentiostat(Princeton Applied Research, U. S. A.). Its output was recorded on a Kipp & Zonen x-t strip chart recorder(BD 111, Holland).

**Fabrication of enzyme electrode.** After dissolving 0.09 g of ferrocene in 10 mL of chloroform, 0.91 g of the graphite powder was added and then dried. By mixing 1.0 g of the produced graphite powder with the solution of EPDM (5.0%) at a 1:1 ratio (wt/wt), electrode material was made. 1 g of this paste was completely mixed with 0.065 g of the ruptured chicken liver tissue. The biosensor was constructed by packing this paste into a 6 mm i/d. and 1 mm depth polyethylene tube having the ohmic con-

tact. It was smoothed by friction on a spatula to make a flat working surface. The LSV's were obtained in the state of the unstirred. Amperometric current was obtained as follows. When the decreasing tendency of the charging current keeps horizontal after applying the step potential on the working electrode, substrate solution is added in 10 mL of 0.1 M NaCl solution. Then the current difference between before and after adding the solution was considered to be the decomposition current of substrate.

## Results and Discussion

When trying to determine the quantity of electricity using the enzyme electrode, electrochemical characterization of constituent materials of the electrode should be precedent. Constituent elements of the electrodes used for this work are 2 to 4. Table 1 shows their combinations to elucidate the electrochemical activities of each component. Here, graphite powder for the conductor, EPDM for the binder, ferrocene for the mediator and liver tissue for the source of enzyme are used. In Figure 1, A-1 shows an LSV obtained with the electrode A in the absence of substrate. It depicts a very large cathodic current above at −300 mV. The appearance of this reduction current is for two plausible reasons. The standard reduction potential of water is −0.828 V (*vs.* SHE). It is probable that the tail of the reduction function of water would have much influence in this part of potential range. During the process of electrolysis at this potential or higher, one may observe air bubbles on the electrode surface by the naked eye. EPDM is a mixture composed of various chemical components whose identities have not yet been elucidated here. Current appearing in the said potential range can be viewed as the reduction current of unidentified components in EPDM. Potential range distorted by side reactions from the high electrode potential should be excluded from experimental consideration. A-2 was an LSV obtained when the experimental range of potential was narrowed down to −300 mV. This does not show any signs of side reactions even though the substrate was added. B-1 and B-2 are LSV's obtained using electrode B in order to examine the electrochemical behavior of the chicken liver tissue. The former was acquired in the absence of substrate and the latter in the presence of substrate. There is little difference between the two LSV's in shape, but the cathodic current and the anodic current are observed above at −200 mV and below at +300 mV, respectively. Those phenomena arise from the addition of liver tissue to the carbon paste. This says that any of the unidentified components contained in the ground liver tissue are electrochemically active in those ranges of potential. Therefore it is reasonable that those two ranges should be excluded from experimental consideration.

On the whole, the current signal increases and stabilizes when the mediator is added. The most essential requirement of electrochemical analysis is that 100% of the signal current should be from the reaction at hand. In cases where the measured quantity involves the current resulting from side reactions, the amperometric analysis is meaningless. The total volume of an enzyme is very bulky and its active site is located far away from the surface of the protein. So it requires very high overvoltage to directly reduce the substrate by the electrons springing up on the electrode surface. The high voltage may generate some unexpected side reactions. In electrochemistry, mediators are used in order to avoid those difficulties. Ferrocene used here is known to have good reversibility of transformation with ferricinium. It conveys the electron from the electrode to the active site without its net reaction at the lower electrode potential (ferricinium$^{+}$ + e$^{-}$ → ferrocene, $E^{o}$ = +0.400 V *vs.* SHE). As a result the decomposition of substrate occurs at the low potential and can effectively contain the side

**Table 1.** Profiles of each electrode for the electrochemical characterization of components in the paste

| Electrode | Each paste contains | ref. |
|---|---|---|
| A | gr (0.5 g) + EPDM (0.5 g) | A in Fig. 1 |
| B | gr (0.5 g) + EPDM (0.5 g) + tis (0.065 g) | B in Fig. 1 |
| C | gr (0.5 g) + EPDM (0.5 g) + tis (0.045 g) | C in Fig. 1 |
| D | gr (0.5 g) + EPDM (0.5 g) + tis (0.045 g) + tis (0.065 g) | D in Fig. 1 |

gr: graphite powder, EPDM: 5% in tolune, tis: chicken liver tissue, fer: ferrocene.

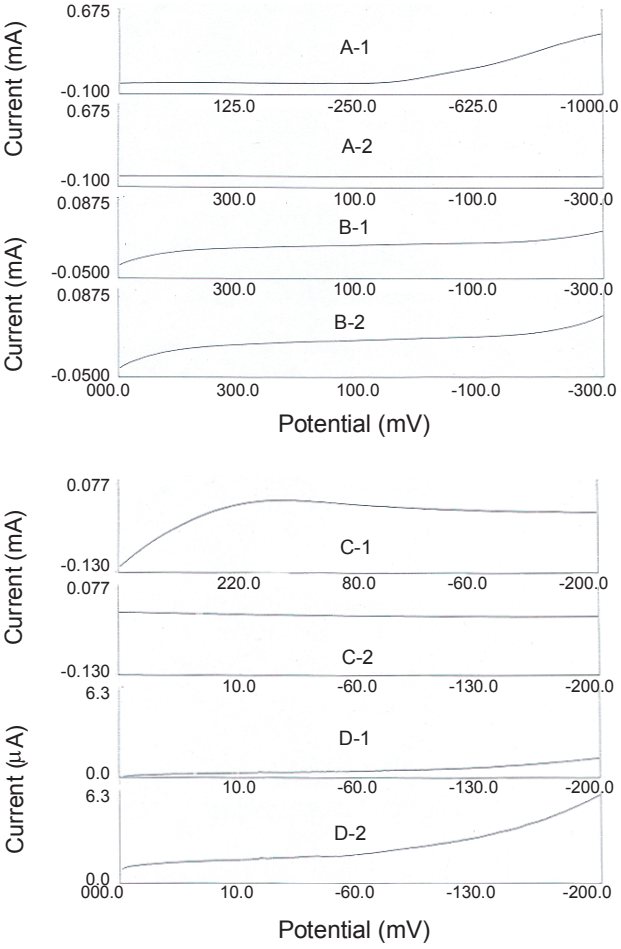


**Figure 1.** Linear sweep voltammograms for seeing through the electrochemical activity of each component in the carbon paste. 1 and 2 were obtained from the solution without and with the substrate (0.02 M $H_2O_2$) respectively. Scan rate: 50 mV/sec.

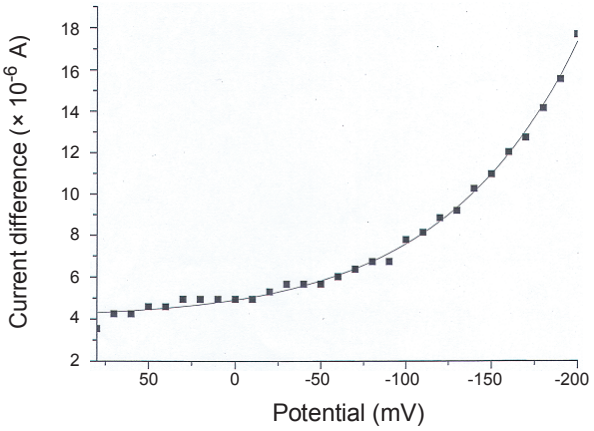


**Figure 2.** Potential dependence of current difference(filled square) between D-1 and D-2 in Figure 1.

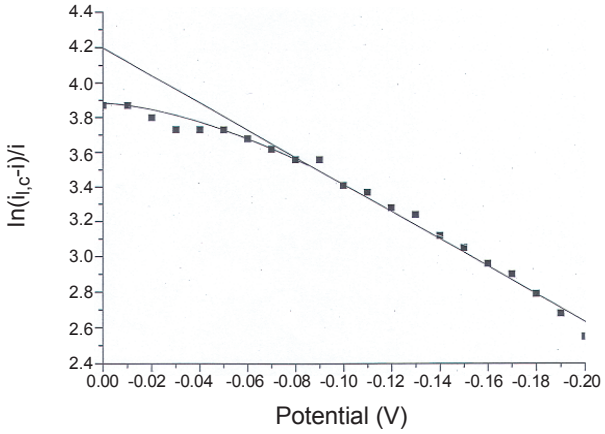


**Figure 3.** Linear plot of ln(i$_{l,c}$ -i)/i *vs.* E.

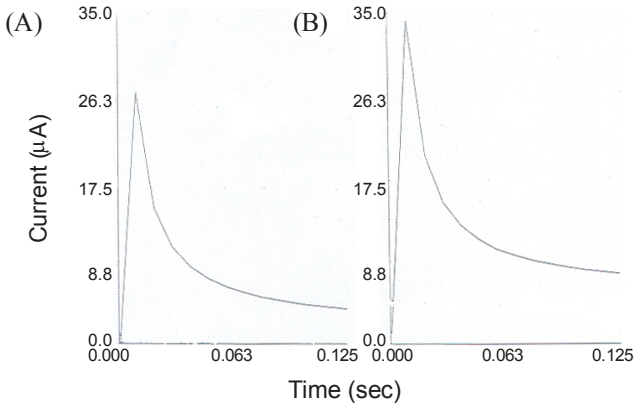


**Figure 4.** Current transient (i *vs.* t) resulting from potential step of magnitude −150 mV (*vs.* Ag/AgCl). A and B were obtained from the solution without and with the substrate (0.02 M $H_2O_2$) respectively.

reactions caused by the high voltage of the electrode. Two LSV's obtained using electrode C in order to examine the electrochemical behavior of ferrocene in this system are C-1 and C-2. The current peak appearing at +166 mV (*vs.* Ag/AgCl) was caused by the addition of ferrocene to the electrode material(C-1). The potential, which is +166 mV from Ag/AgCl, is +363 mV with respect to S.H.E. Considering the overpotential caused by EPDM, this is roughly equal to +0.400 V. C-2 was obtained in the potential range that cancels the electrochemical activity of ferrocene. In spite of the presence of the substrate, it is very horizontal and any signs of side reactions are not seen. D-1 was acquired in the absence of the substrate when the graduation of the current of C-2 was subdivided into microamperes. A small residual current increasing with the electrode potential is observed. The extent of noise like this is unavoidable in electrochemistry. So the experimental range of the electrode potential was restricted to this region. The addition of $H_2O_2$ results in an increase in the reductive current (D-2). The conclusion can be drawn that the current is from the mediation of ferrocene. When the potential range was expanded to −1600 mV, electrode D showed an increase of reduction current similar to A-1 above, particularly at −800 mV. It is evident that the current is due to the direct reduction of $H_2O_2$ by the electrode potential. Electrochemical properties of the electrode materials do not interfere with the analysis of the mediated current in the potential range established above, 80 ~ −200 mV. Therefore there are no obstacles to set this range up as our experimental stage. Figure 2 shows the variation in the difference between D-1 and D-2 with the electrode potential. When the electrochemical reaction is diffusion-controlled in voltammetry, the current-time (voltage) profile is commonly sigmoidal like the polarographic wave. One small part of the wave is illustrated because the confine of the independent variable, electrode potential, can not go beyond -200 mV. Performing the Boltzmann fit gives the functional relation between signal current and electrode potential as follows:

$$i = 3.98 + 239.82/[1 + \exp\{(V + 408.76)/73.79\}]$$

where i is the current density (μA/cm$^2$) and V is the applied potential (mV). When V is infinitely great, i is 243.8 (μA/cm$^2$), which is regarded as limiting current, $i_{l,c}$. The reaction between ferrous ion and hydrogen peroxide occurring in the organism is as follows:

$$Fe^{2+} + H_2O_2 \rightarrow Fe^{3+} + OH^- + OH^{\bullet}$$

This is one electron transfer reaction (n = 1).[23-25] In the case of the irreversible system, kinetic parameters ($i_0$, α, *etc.*) of the electrode reaction may be obtained in the Tafel region. The relation between overpotential, E and ln ( $i_{l,c}$ -i)/i is linear and its slope and intercept are RT/αnF and {RT/αnF}ln ($i_o/i_{l,c}$), respectively. Figure 3 is a graph of ln ($i_{l,c}$ -i)/i *versus* E. Symmetry factor, α and exchange current density, $i_o$, analyzed with the graph in Figure 3 are 0.20 and 3.66 μA/cm$^2$, respectively. The characteristics of electron transfer are dependent on the structure of the electrode surface. In order to gather information on the carbon-solution interface, two current transients (i *vs.* t) of the electrode D were measured by potential step. They are given in Figure 4. A was obtained from an electrolytic solution and B, from 0.02 M $H_2O_2$ in the electrolytic solution. The condenser current decays after the fashion of the 1-st order exponential function. The currents obtained since 0.01 sec after

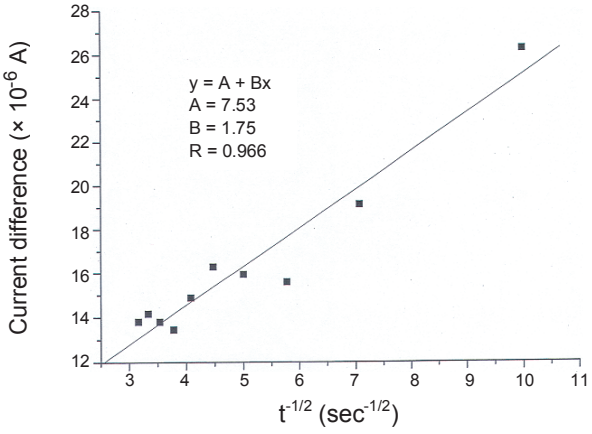


**Figure 5.** Cottrell plot. Current difference between A and B in Figure 4 is plotted with $t^{-1/2}$.

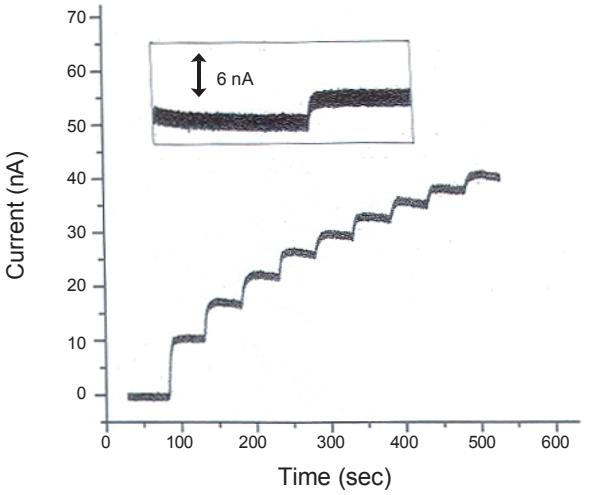


**Figure 6.** Change of the amperogram with the successive additions of 50 μL of 0.1 M $H_2O_2$ to 10 mL of electrolytic solution on electrode D. Inset: an amperogram for the determination of detection limit (60 μL of 0.01 M $H_2O_2$ was added. Operationg potential: −200 mV.

potential excitation were simulated and the functions were extrapolated to t = 0 sec. $i_{max,A}$ and $i_{max,B}$ obtained from those were 167.11 μA/cm$^2$ and 207.74 μA/cm$^2$ at t = 0 sec, respectively. And the time constants, $\tau_A$ and $\tau_B$, were 0.018 sec and 0.019 sec, respectively, which showed very similar tendencies.

When applying a potential step of magnitude E, the decay of the condenser current with time, is

$$i = E/R_s \exp(-t/R_sC_d)$$

where $R_s$ is the solution resistance and $C_d$ is the capacitance of the double layer. The relation is $i = E/R_s$, and $\tau = R_sC_d$ when the capacitor is initially uncharged (q = 0 at t = 0). A in Figure 4 is able to find the value of $R_s$ and $C_d$, which are $8.98 \times 10^2$ Ω and $2.0 \times 10^{-5}$ F respectively. Since the derivation of B from A in Figure 4 comes from the addition of $H_2O_2$ while maintaining the same conditions, one may consider B to be the sum of the charging current (A) and the reduction current of the substrate. That is, the current difference between B and A would be the independent contribution of the substrate. A plot of diffusion current *versus* $t^{-1/2}$, called Cottrell plot, yields a straight line with a slope of $nFAD_oC_o^*/\pi^{1/2}$, where A is the area of the planar electrode, $D_o$ is the diffusion coefficient of the analyte and $C_o^*$ is the bulk concentration. Figure 5 illustrates the Cottrell plot of our system and its slope, $1.75 \times 10^{-6}$ (Asec$^{1/2}$), enabled to calculate $2.58 \times 10^{-12}$ (cm$^2$/sec) as the diffusion coefficient of substrate. Figure 6 is a typical current-time response curve for the successive additions of 50 μL of 0.1 M $H_2O_2$ for the sensor in the stirred 10 mL of the electrolytic solution. This method has the advantage that a steady state of the Faraday current is attained rather quickly because the rates of mass transfer are much larger than those of diffusion. In addition, at steady state, the double layer charging does not enter the measurements. A prominent feature of Figure 6 is that the current is saturated within 15 sec just after the addition of substrate. This means that the enzyme of tissue bound by EPDM is effectively embedded on the electrode surface. Therefore, this fact implicitly tells us that EPDM can be utilized as a binder of graphite powder for biochemical monitoring. An amperogram for determining the detection limit of the electrode used currently is in the window of Figure 6. The detection limit was $1.7 \times 10^{-5}$ M when it gave a signal equal to two times the peak-to-peak noise level of the base line. The detection limits of sol-gel biosensor by A. N. Díaz *et al.*[26] and M. Y. Miao[27] were $6.7 \times 10^{-4}$ M and $3.0 \times 10^{-6}$, respectively. Many kinds of factors affect the detection limit. The examples follow a concentration of mediator, a content of enzyme, pH of solution, temperature and so on. If those are optimized to obtain the highest response, it will be further improved.[28] A calibration curve obtained from the accumulative signal current and substrate concentration in Figure 6 is given in the inset of Figure 7. Calibrations of the enzyme electrode as a function of substrate concentration deviate easily from their linearity even at low concentration. Several explanations are possible for this phenomenon. First of all, it is probable that the enzyme can catalyze at any one of the steps when the dissociation of hydrogen peroxide goes through multi-step reactions. Secondly, various kinds of iso-

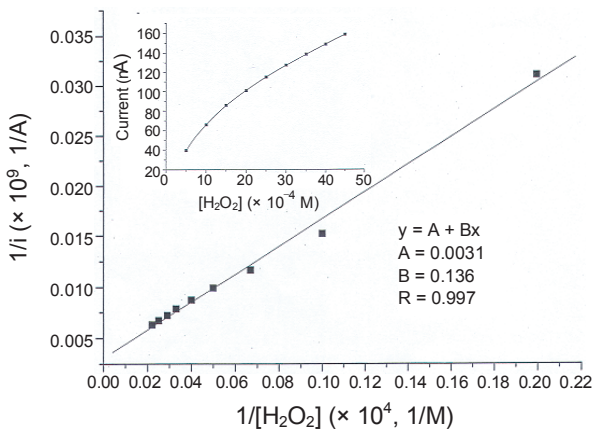


**Figure 7.** Double reciprocal plot of the signal and the substrate concentration. They were calculated cumulatively from Figure 6. Inset: the calibration profile.

enzyme in this system can take part in the hydrogen peroxide dissociation at various rates. Besides, the active sites on the electrode surface are limited in number and the intermediates can be adsorbed or saturated on the sensor surface. Figure 7 is a Lineweaver-Burk plot obtained by taking the reciprocals of both accumulative signals and substrate concentration in Figure 6. The plot shows good linearity with a correlation of 0.997. From this plot, $i_{max} = 3.23 \times 10^{-7}$ (A) and $K_M = 4.39 \times 10^{-3}$ (M). Here a good linearity implies that the decomposition of $H_2O_2$ is from the catalysis of the enzyme contained in chicken liver and says again that EPDM is a recommendable binder of graphite powder.

## Conclusion

The above-stated experimental facts and kinetic parameters show that the enzyme electrode bound with EPDM exerts catalytic power qualitatively and quantitatively. And the robustness acquired by the fast volatility of solvent makes a practical use of the carbon paste electrode possible. These demonstrate that EPDM is recommendable as a binder of graphite powder. Even though the present study has attractive characteristics, such as simple construction and low cost, this biosensor is currently inferior to the spectroscopic method in the aspect of detection limit. If further efforts for the improvement of the detection limit are undertaken side by side, this methodology may compensate for the drawbacks which are common for voltammetries and be suitable for mass production.

## References

1. Cheng, T. J.; Lin, T. M.; Chang. H. C. *Anal. Chim. Acta* **2002**, *462*, 261.
2. Roy, J. J.; Abraham, T. E.; Abhijith, K. S.; Kumar, P. V. S.; Thakur, M. S. *Biosens. Bioelectron*. **2005**, *21*, 206.
3. Gooding, J. J.; Pugliano, L.; Hibbert, D. B.; Erokhin, P. *Electrochem. Com*. **2000**, *2*, 217.
4. Yang, Y. F.; Mu, S. L. *Biosens. & Bioelectron*. **2005**, *21*, 74.
5. Vostiar, I.; Tkac, J.; Sturdik, E.; Gemeiner, P. *Bioelectrochem.* **2002**, *56*, 113.
6. Miscoria, S. A.; Barrera, G. D.; Rivas, G. A. *Sens. Acturators B* **2006**, *115*, 205.
7. Miquel, A. S.; Arben, M.; Salvador, A. *Sens. Acturators B* **2000**, *69*, 153.
8. Olschewski, H.; Erlenkötter, A.; Zaborosch, C.; Chemnitius, G. C. *Enzyme Microb. Technol*. **2000**, *26*, 537.
9. Chen, X.; Zhang, J. Z.; Wang. B. Q.; Cheng, G. J.; Dong, S. J. *Anal. Chim. Acta* **2001**, *434*, 255.
10. Li, Y. C.; Bu, W. F.; Wu, L. X.; Sun, C. Q. *Sens. Acturators B* **2005**, *107*, 921.
11. Tingry, S.; Innocent, C.; Touil, S.; Deratani, A.; Seta, P. *Mater. Sci. Eng. C* **2006**, *26*, 222.
12. Morrin, A.; Guzman, A.; Killard, A. J.; Pingarron, J. M.; Smyth, M. R. *Biosens. Bioelectron*. **2003**, *00*, 1.
13. Wang, J.; Mo, J. W.; Li, S. F.; Porter, J. *Anal. Chim. Acta* **2001**, *441*, 183.
14. Yoon, K. J. *Anal. Sci. Tech*. **2003**, *16*, 504.
15. Yoon, K. J. *Bull. Korean Chem. Soc*. **2004**, *25*, 997.
16. Yoon, K. J. *J. Kor. Chem. Soc*. **2004**, *48*, 654.
17. Choi, S. Y.; Yoon, K. J. *Elastomer* **2006**, *41*, 231.
18. Yoon, K. J. *Anal. Sci. Tech*. **2007**, *20*, 49-54.
19. Yoon, K. J. *Bull. Korean Chem. Soc*. **2008**, *29*, 2264.
20. Lee, B. G.; Rhyu, K. B.; Yoon, K. J. *Bull. Kor. Chem. Soc*. **2009**, *30*, 2457.
21. Lee, B. G.; Rhyu, K. B.; Yoon, K. J. *J. Ind. Eng. Chem.* **2010**, *16*, 340.
22. Brydson, *Rubbery Materials and Their Compounds*; Elsvier Applied Science: London and New York, 1988; p 147.
23. Mansouri, A.; Makris, D. P. M.; Kefalas, P. *J. Pham. Bio. Anal*. **2005**, *39*, 22.
24. Graft, E; Mahoney, J. R.; Bryant, R. G.; Eaton, J. W. *J. Biol. Chem*. **1894**, *259*, 3620.
25. Henle, E. S.; Linn, S. *J. Biol. Chem*. **1997**, *272*, 19095.
26. Díaz, A. N.; Peinado, M. C. R.; Minguez, M. C. T. *Anal. Chim. Acta* **1998**, *363*, 221.
27. Miao, Y.; Tan, S. N. *Anal. Chim. Acta* **2001**, *437*, 87.
28. Yoon, K. J.; Pyun, S. Y. Kwon, H. S. *J. Kor. Chem. Soc*. **1997**, *41*, 343.